DESIGN OF A CW 1 THz GYROTRON (GYROTRON FU CW III) USING A 20 T SUPERCONDUCTING MAGNET

研究報告 2

DESIGN OF A CW 1 THz GYROTRON (GYROTRON FU CW III) USING A 20 T SUPERCONDUCTING MAGNET

La Agusu, T. Idehara, H. Mori, T. Saito, I. Ogawa and S. Mitsudo

Research Center for Development of Far-Infrared Region, University of Fukui, 3-9-1 Bunkyo, Fukui-shi 910-8507, Japan

Abstract

Design of a CW 1 THz gyrotron at second harmonic operation using a 20 T superconducting magnet has been described. The mode competition analysis is employed to investigate operation condition of second harmonic mode which is being excited at the frequency ranging from 920 GHz to 1014 GHz. The output power up to 250 watt corresponding to the efficiency of 4.16 percent could be achieved by using beam energy 30 kV, 200 mA. The important advantage of this gyrotron is that the single mode excitation at second harmonic, at extremely high frequency radiation could be maintained at the high current. It opens possibility to realize a high power radiation at 1 THz. The gyrotron is under construction at FIR Center, University of Fukui.

1. Introduction

A gyrotron is an important source of short wavelength coherent radiation. Gyrotron development is being advanced in two ways. The major way is development of high power, millimeter wave gyrotrons for heating and current drive for fusion plasma. It is going world-widely and has achieved around 1MW output power for long pulse operation (longer than several tens second or quasi CW) at the frequency of 170 GHz or 140 GHz [1-4]. On the other hand, medium power, high frequency gyrotrons are being developed in several institutions in the world [5-7]. In the cases, high magnetic field and higher harmonic operations are used for increasing operation frequency. Such gyrotrons have already covered wide frequency range in millimeter to submillimeter wavelength region and been applied as submillimeter wave radiation sources for wide fields including plasma diagnostics [8], electron spin resonance (ESR) spectroscopy [9,10], nuclear magnetic resonance (NMR) spectroscopy [11], new medical technology [12], and so on.

Terahertz sources corresponding to frequencies between 300 GHz and 3 THz have considerably attention for use in many fields, such us the material sciences, solid-state physics, molecular analysis, atmospheric research, biosciences, medical treatment, food inspection, and airport security. Many sources and mechanisms have investigated and successfully give generation in terahertz regime. Gyrotrons has promising advantage over the conventional vacuum electron devices for the THz source. Gyrotron oscillators and amplifiers rely on a resonance between the modes of an interaction structure (such as transverse electric modes of a cylindrical cavity) and electron beam in a magnetic field. The resonator can be overmoded with the physical dimensions are much larger than the operating wavelength. This permits high peak and average power operation even at elevated frequencies without risk of damage to the interaction structure. In the case of the conventional vacuum electronic devices such as the klystron and traveling wave tube (TWT), the physical dimensions of their interaction structures scale are comparable with wavelength. As the result, increasing in power density with increasing frequency limits the reliability and utility of these devices at high frequency above 140 GHz.

The frequency of a gyrotron corresponds to the magnetic field intensity and the harmonic number. Operating the gyrotron at the harmonic can remove the problem of using high field intensity where the nth harmonic will deliver n times the fundamental frequency for a given magnetic field. For example, to achieve 1 THz radiation, a gyrotron operating at second harmonic requires only 19 T corresponding to 502 GHz fundamental frequency if one uses 30 kV of electron energy. However, harmonic interaction is inherently less efficient than the fundamental interaction due to elevated ohmic losses. It also needs more careful design and selection of parameter in order to solve mode competition with lower harmonic.

Our gyrotrons developed in FIR FU named Gyrotron FU Series belongs to the second type gyrotrons, that is, medium power high frequency gyrotrons. The series has achieved following items, 1) frequency step-tuneability in wide range in millimeter to submillimeter wavelength region (from 38 to 889 GHz), 2) highest frequency (889 GHz) corresponding to the wavelength of 377μm by using second harmonic operation at the field intensity of around 17 T, 3)

modulation of amplitude and frequency of the output, 4) stabilization of amplitude and frequency, 5) higher harmonic operations up to fifth and 6) high-purity mode operations at many cavity modes by installation of a carefully designed cavity [13]. Also, we have achieved mode conversion from circular waveguide modes to a Gaussian mode for applications of our gyrotrons to many fields [14]. Recently, the breakthrough of 1 THz in pulse operation was achieved in our center [15].

For convenience of the application, CW gyrotrons (Gyrotron FU CW Series) is being developed. Gyrotron FU CW I have been developed and succeeded in the CW operation at 300 GHz under high power of 1.8 kW [16]. The Gyrotrons FU CW II is being developed with the parameter, 395 GHz-100 W under CW operation [17]. These gyrotrons will be used for development of high power THz technologies, for example, plasma diagnostics, DNP-NMR, etc.

In this paper, we report the design of a CW gyrotron with an output power at 100 watt at the frequency of 1 THz. It is the third CW gyrotron in FIR FU, Gyrotron FU CW III, with a 20 T superconducting magnet. It will be operated at second harmonic. The superconducting magnet employing combination of NbTi and Nb_3Sn superconductor wires which has been designed and constructed in JASTEC Co. The operating test has been successfully carried out. The design consideration and simulation result of gyrotron will be described.

2. Gyrotron design considerations

The goal of this design is to successfully generate hundreds watts level of 1 THz CW power at the second harmonic. The design of the 1 THz CW gyrotron oscillator is based on a previous pulse 1 THz gyrotron oscillator built at FIR Center, University of Fukui [15]. The experimental test using a 21 T pulse magnetic system has been carried out with the radiation frequency ranges from 395 GHz to 1.014 THz. Operational characteristic of this design includes the ability to excite a second harmonic cavity mode without competition with the fundamental modes, at a high power level in THz regime. A cross-sectional view of the CW 1 THz gyrotron system is shown in Fig. 1. The axes of the gyrotron tube and electron beam are lie along the center of axis of the bore of a 20 T superconducting magnet. There are two pumping bores. First is located near the electron gun to assure the vacuum condition inside the tube. Second is placed after the collector to pump out the out-gas from the electron collector as well as the resonator. In the continuous-wave (CW) operation, temperature of cavity increases during the operation. It has been observed in the experiment that there was an influence of increasing cavity temperature on the shift of the frequency and output power of CW gyrotron [18,19]. The cooling system surrounding the cavity is necessary. The water jacket with a constant flow is installed surrounding the whole gyrotron tube, including the electron collector, to maintain the tube temperature at a permissible level for stable operation of gyrotron. In the collector, the rest electron beam energy is collected. The electron collector also serves as the microwave waveguide to the output window. To allow pumping out at the collector end, the small holes are made with diameter less than the wavelength.

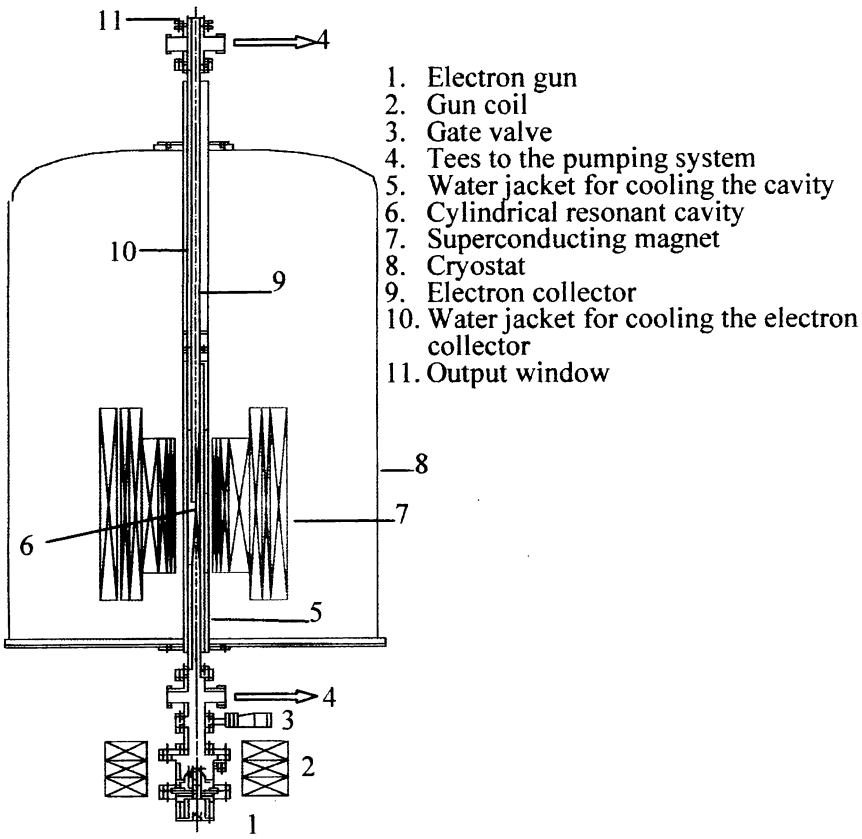

Fig. 1 The cross-sectional view of the cylindrically symmetric 1 THz CW gyrotron tube. The gyrotron tube is approximately 2.5 m long and magnet bore diameter is 5 cm.

The total length of tube including the collector is 2.5 m. Sets of two stages for horizontal alignment are located both under and upper part of the cryostat and are used to align the gyrotron tube with respect to the magnetic field of the superconducting magnet, thereby aligning the axis of the electron beam. The gyrotron tube is demountable which enables to change some parts of it.

A. Superconducting magnet

The superconducting magnet with inner bore diameter of 5 cm, consists of eight part cylindrically symmetry coils with total winding of 30676. There are four Nb_3Sn coils and NbTi coils. The expected maximum field intensity is 20 T at the current of 290 A. Inhomogeneity for 2 cm from the center of magnet is only 0.11 percent. The distance between the emitter of electron gun and the center of superconducting coil is approximately 82 cm. The superconducting magnet provides maximum field intensity of 0.21 T at the emitter.

B. Electron gun

The electron gun is a triode magnetron injection gun which has been used for several gyrotrons in our center, Gyrotron FU V [20], 1 THz pulse gyrotron [15], and Gyrotron FU CW II (395 GHz) [17]. It has the following

geometry: the radius of the emitter is, the distance between emitter and the anode is 2.78 mm. The electron gun properties for new operation condition has been investigated by means of EPOSR code [21], which allows taking into account the real space distribution of magnetic and electric field within two-dimensional model. The space charge force as well as magnetic field was also included into numerical model.

Additional coil called 'gun coil' are necessary to be installed surrounding the electron gun centered at the emitter in order to adjust the beam parameters as well as the beam quality at the entrance of the cavity. Three additional coils cooled by water are installed as gun coil. The maximum field intensity provided by the gun coil is 0.13 T at the current of 300 A. The beam radius for excitation of desired operating modes at the second harmonic is 0.35 mm corresponding to 0.11 T. The superconducting magnet produces 0.21 T at the cathode. The gun coil behaves as the counter running coil to produce field intensity in opposite direction toward the main field produced by the superconducting magnet. It allows us to adjust the beam radius from 0.28 mm to 0.58 mm.

Numerical simulation shows that the angle of magnetic field to the emitter is 15.7, so the gun forms boundary beam. The nominal pitch factor α = 1.1, the velocity spread, $\delta v_{\perp}$ is about 10 percent. Fig. 2 shows the trajectory of three electrons near the cathode nose.

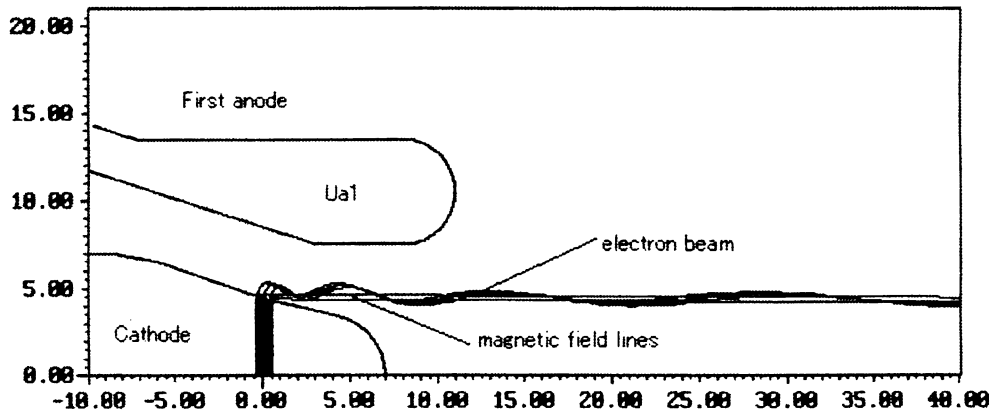

Fig. 2 Electron trajectory near the cathode.

C. Interaction Cavity

The resonant gyrotron interaction structure is a cylindrical cavity with length and radius are 10 mm and 1.95 mm. It is joined to a linearly uptapered section with a slope 22.3° and a linearly downtapered section with the slope of 5.1°. Fig. 3 shows the cross-section of cavity and the axial profile of the desired cavity mode, $TE_{4,12}$. The material of the gyrotron cavity is copper. Based on the cold-cavity calculation, the frequency and total Q-factor are approximately 1013.67 GHz and 23720, respectively

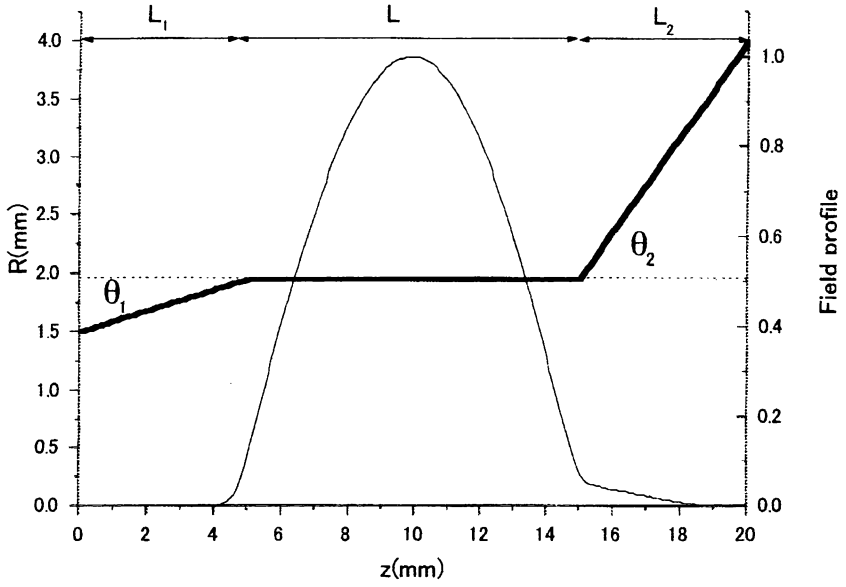

Fig. 3 The cross- section of a 1 THz GHz gyrotron cavity with the axial field profile for the cavity mode $TE_{4,12}$ at second harmonic. Input taper: L_1 = 5 mm, $\theta_1 = 5.1^\circ$; Middle section R = 1.95 mm, L = 10 mm; output taper: L_2 = 5 mm, $\theta_2 = 22.3^\circ$.

3. Mode competition

Mode competition study is needed for establishing single excitation region of second harmonic mode by removing the competition with the fundamentals and other second harmonic modes. Mode competition can be studied by the self-consistent, multimode, time-dependent system of equations [22]:

$$\frac{\partial p}{\partial \varsigma} + i\left(|p|^2 - 1\right)p = i\sum_s \left(p^*\right)^{n_s - 1} f_s \exp\left[i\left(\Delta_s \varsigma + \psi_s\right)\right]$$

$$\frac{\partial^2 f_s}{\partial \varsigma^2} - i n_s \frac{\partial f_s}{\partial \tau} + n_s \delta_s = I_s \frac{1}{4\pi^2}\int_0^{2\pi}\int_0^{2\pi} p^{n_s} d\theta_0 \exp\left[-i\left(\Delta_s \varsigma + \psi_s\right)\right] d\phi \qquad (1)$$

Here $\Delta_s = \frac{2}{\beta_\perp^2}\left(\frac{\overline{\omega_s} - n_s\omega_c}{\omega_c}\right)$ is the frequency mismatch, is the RF field in resonator, $\psi_s = 8\beta_\parallel^2\beta_\perp^{-4}\left(\overline{\omega_s} - \omega_c\right)\omega_c^{-1}\tau + \left(n_s \mp m_s\right)\phi$ is the phase of the mode, m_s and ϕ are the azimuthal index and coordinate, respectively, $\tau = \frac{1}{8}\beta_\perp^4\beta_\parallel^{-2}\omega_c t$ is the dimensionless time, t is time, $\delta_s = 8\beta_\parallel^2\beta_\perp^{-4}\left(\overline{\omega_s} - \omega_{cut,s}(\zeta)\right)\omega_c^{-1}$ describes variation of the cut-off frequency along the resonator axis, $\overline{\omega_s}$ is the cut-off frequency at the exit from the resonator, I_s is the dimensionless current which includes the RF field and electron beam coupling. The subscript s refers to the s-th mode.

The first equation in the system (1) has to be supplemented by the

initial condition $p(0)=\exp(i\theta_0)$, $0\le\theta_0<2\pi$ and the second equation by $f(\zeta,0)=f_0(\zeta)$, where $f_0(\zeta)$ is RF field profile obtained in the cold-cavity approximation. The boundary condition for the second equation of the system (1) can be written as usual

$$f_s(\zeta_{out},\tau)=\frac{i}{k_s}\frac{\partial f_s(\zeta,\tau)}{\partial\zeta}\Big|_{\zeta=\zeta_{out}}, \tag{2}$$

where $k_s=2c\beta_{\|}\beta_{\perp}^{-2}\omega_c^{-1}\left[\bar{\omega}_s^2/c^2-\chi_s^2(\zeta)/R_{cav}^2(\zeta)\right]^{1/2}$ is the dimensionless longitudinal wave number, χ_s is the eigenvalue of the mode, and R_{cav} is the cavity radius.

The electron efficiency of gyrotron can be written as

$$\eta=\frac{\alpha^2}{1+\alpha^2}\eta_{\perp}, \tag{3}$$

where $\eta_{\perp}$ is the perpendicular efficiency given by the relation:

$$\eta_{\perp}=1-\frac{1}{2\pi}\int_0^{2\pi}|p(\zeta_{out})|^2 d\theta_0, \tag{4}$$

and $\alpha=\beta_{\perp}/\beta_{\|}$ is the velocity ratio (pitch factor) of the electron.

4. Simulation Results

A. Starting current

Fig. 4 shows the starting current of each cavity mode as function of field intensity ranging from 14.5 T to 20 T. The electron beam parameters are used in calculation are the following: beam voltage is 30 kV, beam radius is 0.4 mm, and pitch factor is 1.1. It enables us to identify the candidate for second harmonic operation at different frequency. It is seen in Fig. 4 that the starting current of $TE_{4,12}$ mode at second harmonic do not overlap with the fundamentals. Some other mode such us $TE_{5,11}$ and $TE_{8,9}$ tend to be excited without competition with the fundamental by adjusting beam current, beam radius, and field intensity. Mode competition calculation will be used to confirm single excitation of these modes.

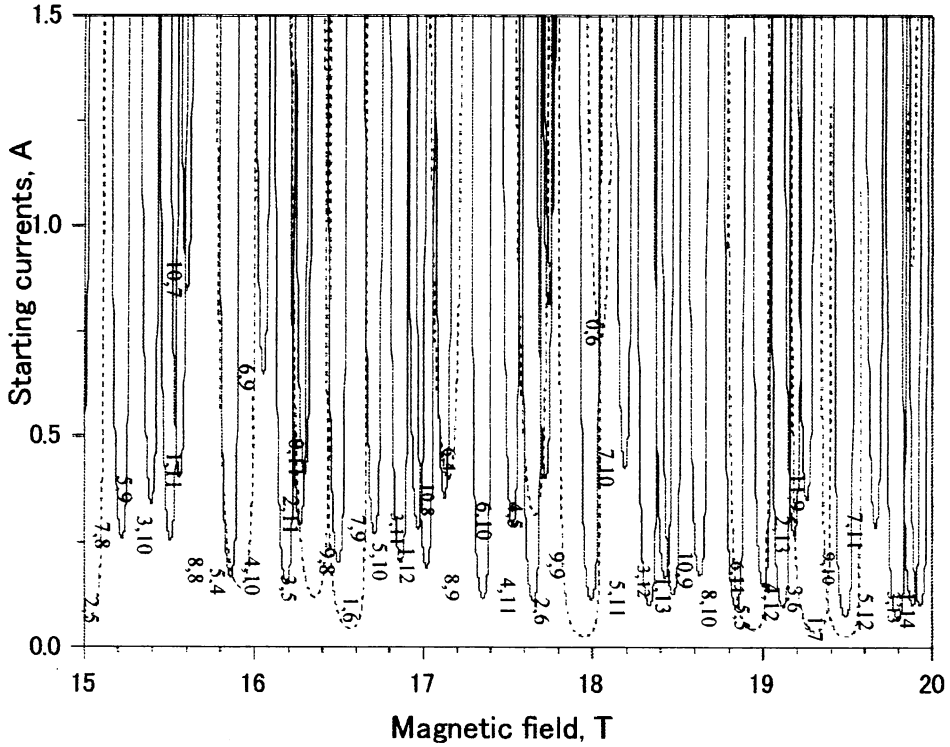

Fig. 4 Starting current of the cavity mode. Here, Vc = 30 kV, R_b = 0.4 mm, and α = 1.1

B. Mode competition scenario

Operation condition of the cavity modes at second harmonic are investigated using mode competition scenario by means of multi-mode time-dependent self-consistent equation of the normalized perpendicular momentum and field amplitude in Eq. (1). Partial differential equations in Eq. (1) are solved by using Runge-Kutta method. Number of electron and phase are 25 and 15, respectively to solve the integral in second part of Eq. (1). This calculation allows taking into account up to seven cavity modes with different harmonic. Calculation are performed for a range of field intensity, with 0.01 T step in order to determine operation condition of cavity mode at the THz regime. At each step, equation (1) is solved for 75 ns of interaction time with 0.1 ns time step. The frequency, initial field profile, and Q-factor as the input

of mode competition calculation are taken from cold-cavity calculation. Normalized initial amplitude of all modes is given 0.01. The final amplitude of each mode is recorded with the corresponding field intensity. At the same time the electron efficiency and output power can be calculated by using of Eq. (3).

Fig. 5 shows calculation result for field intensity ranging from 18.65 T to 19.4 T. The beam parameters used in calculation are cathode voltage 30 kV, beam radius of 0.35 mm, and pitch factor of 1.1 (see Table I). There are six cavity modes potentially could be excited in this magnetic field range (see Table II), i.e. the second harmonic mode $TE_{4,12}$ (f = 1013.67 GHz), $TE_{8,10}$ (f = 999.15 GHz), $TE_{6,11}$ (f = 1007.68 GHz), and $TE_{2,13}$ (f = 1017.23 GHz); and the fundamentals $TE_{5,5}$ (f = 503.64 GHz) and $TE_{3,6}$ (f = 513.35 GHz). Among those modes, only 4 cavity modes: $TE_{8,10}$, $TE_{5,5}$, $TE_{4,12}$, and $TE_{3,6}$ are excited in different magnetic field. It is seen in Fig. 5 that the desired second harmonic cavity modes $TE_{4,12}$ at 1013.67 GHz and $TE_{8,10}$ at 999.15 GHz are excited without competition with the fundamentals. The field intensity for single mode operation of $TE_{4,12}$ is ranged from 19.0 T to 19.1 T. It has been confirmed by using a THz gyrotron with a pulse magnet [15]. In addition, $TE_{8,10}$ at second harmonic could be excited at field intensity ranging from 18.7 T to 18.8 T.

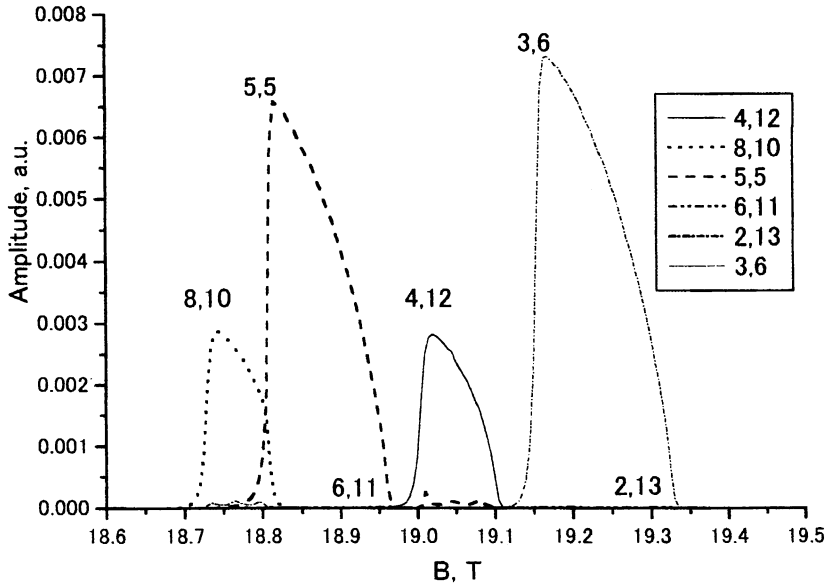

Fig. 5 Amplitudes of cavity modes at the final stage of mode competition calculation (t = 75 ns) as functions of magnetic field. There are six cavity modes are included in calculation. Here, the beam parameters are taken from Table I.

Table I. Parameters of electron beam

Vc (kV)	I_b(A)	R_b(mm)	α
30	0.2	0.35	1.1

Table II List of modes are included in the calculation at 18.65 T < B < 19.4 T

TEmn Mode		Frequency (GHz)	Q	Harmonic number	Rotation
m	n				
4	**12**	**1013.67**	**23720**	**2**	**+**
8	**10**	**999.15**	**22859**	**2**	**-**
6	11	1007.68	23278	2	+
2	13	1017.23	23931	2	+
3	6	513.35	10668	1	+
5	5	503.64	10163	1	-

Fig. 6 shows time evolution of amplitude at B = 19.05 T in Fig 5. The total electronic power and efficiency are 0.77 kW and 12.8 percent. It should be noted here that the calculation did not take into account the velocity spread effect and ohmic losses.

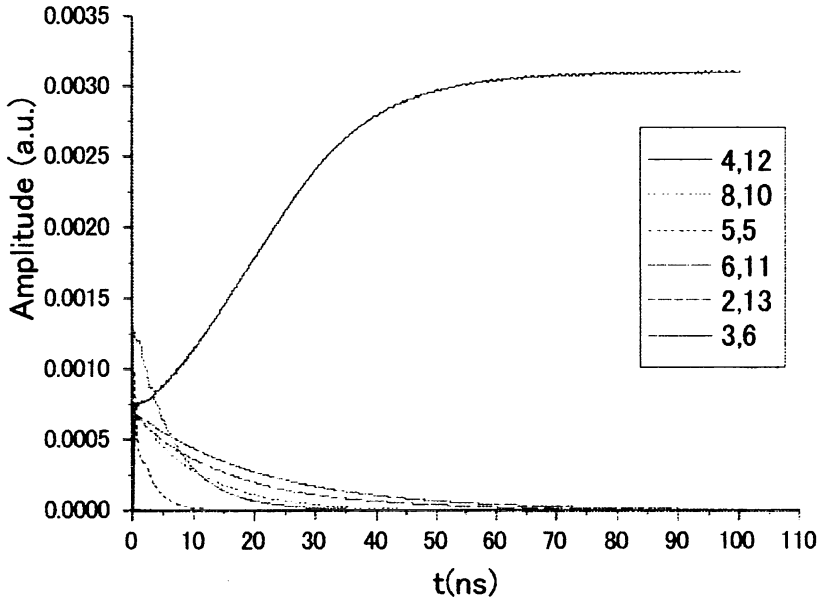

Fig. 6 Time evolution of mode amplitude at B = 19.05 T where the $TE_{4,12}$ suppressed other fundamental and second harmonic modes.

Result of mode competition at B = 19.05 T by increasing beam current is shown in Fig. 7 with corresponding efficiency and electronic power in Fig. 8. We have extended calculation even up to 1.8 A and $TE_{4,12}$ completely suppress other fundamental and second harmonic mode. The important advantage of this operating mode is that the single mode excitation at second harmonic, at extremely high frequency radiation could be maintained at high current. It opens possibility to realize a high power radiation at 1 THz.

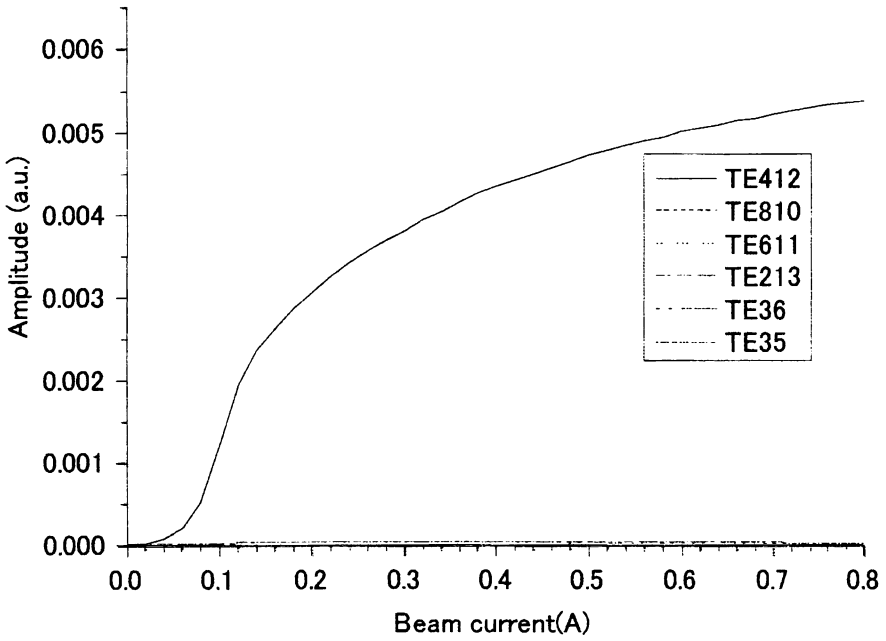

Fig. 7 Final amplitude of mode vs beam current at B = 19.05 T and other parameters in Tables I and II.

Operation condition of the cavity mode at 17.75 T < B < 18.35 T is illustrated in Fig. 9. Parameters used in this calculation are listed in Table I. Four cavity modes at second harmonic and one cavity mode at fundamental are included in mode competition calculation (see in Table III). The most dangerous mode is the fundamental, $TE_{2,6}$ at 477.65 GHz. As a result, $TE_{2,6}$ covers a wide regime of field intensity from 17.75 T to 18.2 T and then it is followed by excitation of $TE_{5,11}$ at 972.25 GHz ranging from 18.25 T to 18.35 T of field intensity. The $TE_{5,11}$ mode at second harmonic is the second candidate for THz radiation. The radiated output power is 0.26 kW with corresponding efficiency of 4.3 percent. First trial of experiment will be carried out at this point and the desired operating mode at second harmonic which can be excited without competition with the fundamental mode is $TE_{5,11}$. Then finally it will be operated at 19 T and higher.

Table III List of cavity mode used in calculation at 17.75 T < B < 18.35 T

TE_{mn} Mode		Frequency (GHz)	Q	Harmonic number	Rotation
m	n				
1	13	979.66	23165	2	+
3	12	977.20	23018	2	-
5	**11**	**972.25**	**22724**	**2**	+
9	9	954.42	21659	2	-
2	6	477.65	9617	1	+

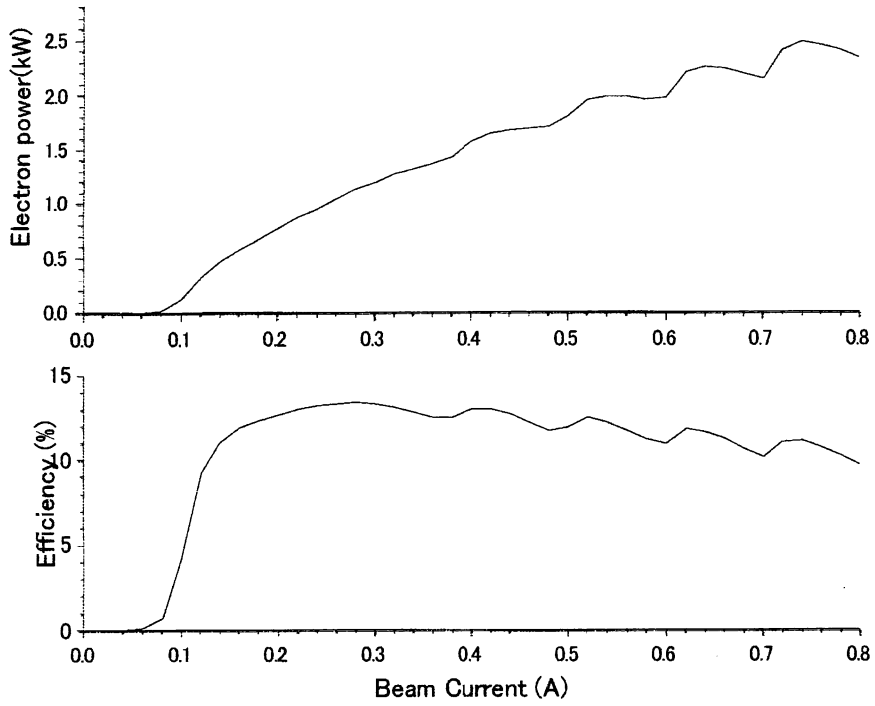

Fig. 8 The electronic power and efficiency for increasing beam current corresponding to the result in Fig. 7.

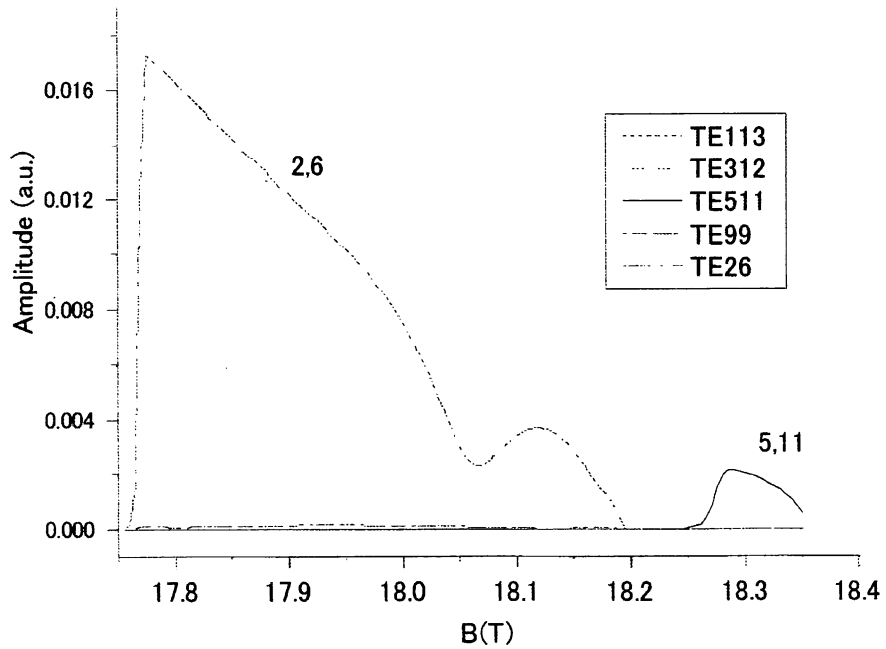

Fig. 9 Amplitude of modes at the final stage of calculation in mode competition scenario (t = 75 ns) for different magnetic field. The regime of single mode excitation of $TE_{5,11}$ at second harmonic is specified.

Fig. 10 shows the mode competition result for field intensity ranging from 17.1 T to 17.4 T, where the second harmonic mode $TE_{8,9}$ is operated at 920.61 GHz without any disturbance from the fundamentals. Here, the beam

parameters are the same as in previous calculations (see in Table I). The radiated power when B = 17.3 T is 0.68 kW corresponding to the efficiency of 11.4 percent (see in Fig. 11).

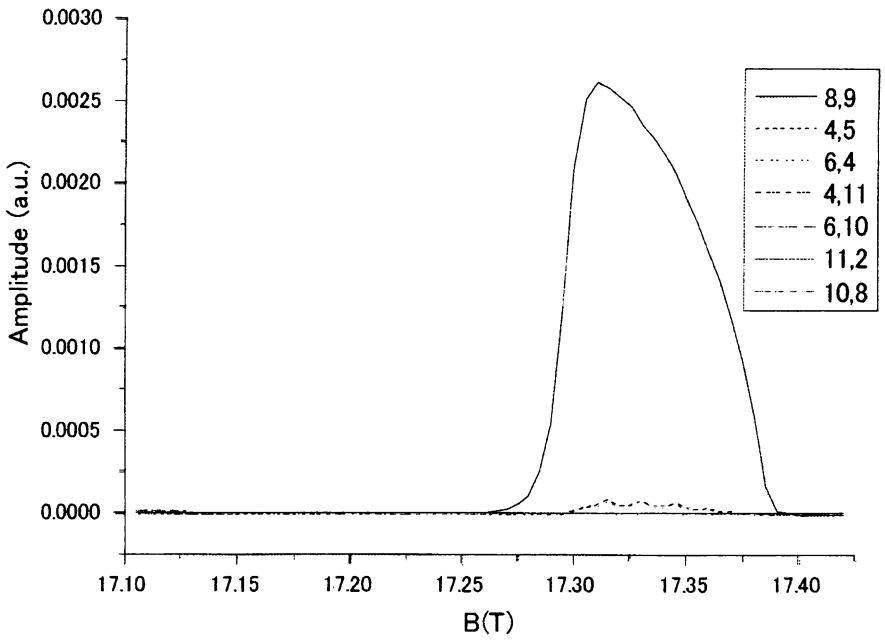

Fig. 10 Amplitude of modes at the final stage of calculation in mode competition scenario (t = 75 ns) as functions of magnetic field. $TE_{8,9}$ mode at second harmonic dominates the region 17.27 T < B< 17.4 T. Operating modes in Table IV are taken into account in the competition. Beam parameters are taken from Table I.

Table IV List of cavity modes in mode competition for specifying operating condition of the desired mode $TE_{8,9}$.

TE_{mn} Mode		Frequency (GHz)	Q	Harmonic number	Rotation
m	n				
8	**9**	**920.61**	**21087**	**2**	-
1	12	902.75	21443	2	-
10	8	908.33	20350	2	-
6	10	929.90	21644	2	-
4	11	936.40	22032	2	-
4	5	469.90	9220	1	-
6	4	456.24	8547	1	+

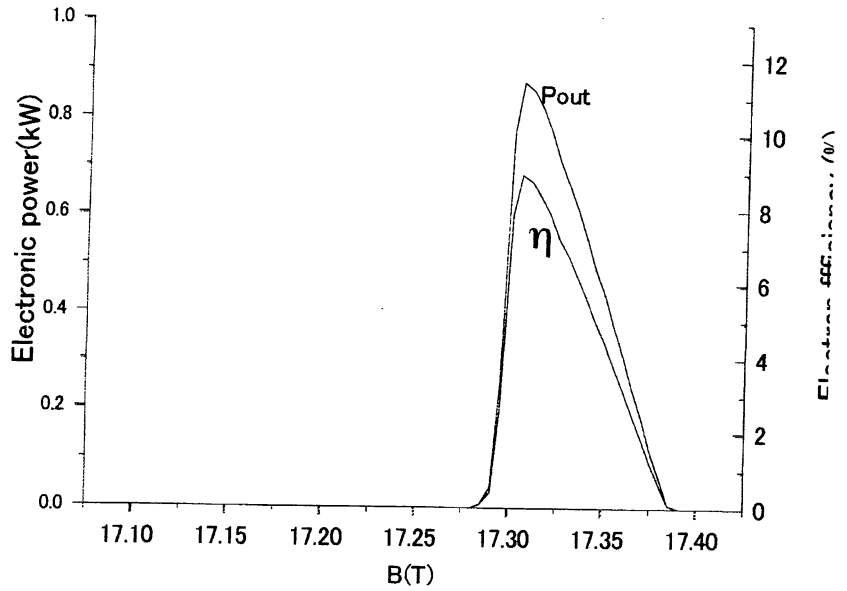

Fig. 11 The electronic power and efficiency vs magnetic field corresponding to the result in Fig. 10.

C. Ohmic Losses

The main source of power losses in second harmonic operation gyrotron is the Ohmic losses. The diffractive Q factor (Q_{diff}) increases significantly in the second harmonic, especially in the case of larger tapering angle ($\theta > 5^{o}$). In the case, the Q_{diff} exceeds the minimum diffractive Q factor ($4\pi L/\lambda$), where L and λ are the cavity length and the wavelength. The Ohmic losses in cavity described by the ratio of Q/Q_{diff} decreases the efficiency in a factor of $1\text{-}Q/Q_{diff}$. Table V shows the detail Q factor and Ohmic losses as well as total output power and efficiency after taking into account Ohmic losses effect for operation at second harmonic. Listed four modes are excited without competition with the fundamental. It is seen in Table V that effect of Ohmic losses is significantly decreasing the output power of gyrotron. It is reasonable because we are using high Q cavity to decrease the starting current in order to minimize competition with the fundamental.

Table V Output power calculation by taking into account the Ohmic losses

	$TE_{4,12}$	$TE_{8,10}$	$TE_{5,11}$	$TE_{8,9}$
Frequency, GHz	1013.67	999.15	972.25	920.61
Qdiff	72208	69590	67075	60242
Qohm	35324	34041	34367	32443
Q	23720	22859	22724	21087
Electronic power, kW (Pout + Pohm)	0.77	0.75	0.26	0.68
Electronic efficiency, %	12.8	12.5	4.3	11.4
Ohmic losses: 1-Q/Qdiff, %	67.15	67.15	66.12	64.99
Total output power, kW	0.25	0.25	0.09	0.24
Total efficiency, %	4.16	4.16	1.5	4.0

5. Gyrotron parameters

With the perspective of establishing high power level in CW at the THz regime, the detailed design of such tube has been completed. The gyrotron is schematized in Fig. 1, and the main characteristics are presented in Table VI. The calculation shows that the operating modes could be excited without competition with the spurious mode. Gyrotron can emit high frequency radiation at second harmonic without utilizing the high-pass filter to suppress the fundamental. It could be a promising design for realizing high power source at 1 THz. The output power of 250 watt level is expected with high stability at super high frequency operation by solving mode competition problem.

Table VI Summarizing the gyrotron parameters.

Frequency	1013.67 GHz	999.15 GHz	972.25 GHz	920.61 GHz
Operating mode	$TE_{4,12}$	$TE_{8,10}$	$TE_{5,11}$	$TE_{8,9}$
Magnetic field	19.05 T	18.78	18.3 T	17.35 T
Cavity radius	1.95 mm			
Cavity length	10 mm			
Cathode voltage	30 kV	30 kV	30 kV	30 kV
Beam current	200 mA	200 mA	200 mA	200 mA
Beam radius	0.35 mm	0.35 mm	0.35 mm	0.35 mm
Pitch factor	1.1	1.1	1.1	1.1
Q_{diff}	72208	69590	67075	60242
Q_{ohm}	35324	34041	34367	32443
Total Q-factor	23720	22859	22724	21087
Electronic power (Pout + Pohm)	0.77 kW	0.75 kW	0.26 kW	0.68 kW
Electronic efficiency	12.8 %	12.5	4.3 %	11.4 %
Ohmic losses: $1-Q/Q_{diff}$	67.15 %	67.15 %	66.12 %	64.99 %
Total output power	0.25 kW	0.25 kW	0.09 kW	0.24 kW
Total efficiency	4.16 %	4.16 %	1.5 %	4.0 %
Cathode radius	4.5 mm			

6. Conclusion

Design of a CW 1 THz gyrotron at second harmonic operation using a 20 T superconducting magnet has been described. The mode competition analysis is employed to investigate operation condition of second harmonic mode which is being excited at the frequency ranging from 920 GHz to 1014 GHz. The output power up to 250 watt corresponding to the efficiency of 4.16

percent could be achieved by using beam energy 30 kV, 200 mA. The important advantage of this gyrotron is that the single mode excitation at second harmonic, at extremely high frequency radiation could be maintained at the high current. It opens possibility to realize a high power radiation at 1 THz. The gyrotron is under construction at FIR Center, University of Fukui.

Acknowledgement

This work was supported partially by Special Fund for Education and Research from the Ministry of Education, Culture, Sports, Science and Technology of Japan.

References

[1] G. Dammertz, S. Alberti, A. Arnold, E. Borie, V. Ercmann, G. Gantenbein, E. Giguet, R. Heidinger, J. P. Hogge, S. Illy, W. Kasparek, K. Koppenburg, M. Kuntze, H. P. Laqua, G. LeCloarec, Y. LeGoff, W. Leonhardt, C. Lievin, R. Magne, G. Michel, G. Mueller, G. Neffe, B. Piosczyk, M. Schmid, K. Schwoerer, M. Thumm, and M. Q. Tran, "Development of a 140-GHz 1-MW continuous wave gyrotron for W7-X stellarator," IEEE Trans. Plasma Sci., **30**, 808-818 (2002).

[2] M. Thumm, "MW gyrotron development for fusion plasma applications," Plasma Phys. Control. Fusion, **45**, A143 - A161 (2003).

[3] V. E. Zapelov, G. G. Denisov, V. A. Flyagin, A. S. Fix, A. N. Kuftin, A. G. Litvak, M. V. Agapova, V. N. Ilyin, V. A. Khmara, V. E. Myasnikov, V. O. Nichiporenko, I. G. Popov, S. V. Usachev, V. V. Alikaev, and V. I. Ilyin, "Development of 170 GHz/1 MW Russian gyrotron for ITER," Fusion Eng. Des., **53**, 377-385 (2001).

[4] K. Sakamoto, A. Kasugai, R. Minami, K. Takahashi, N. Kobayashi, T. Imai, "Development of high power 170 GHz gyrotron for ITER," Conf. Diggest of the 2004 Joint 29th Int. Conf. on Infrared and MM Waves and 12th Int. Conf. on terahertz electronics, ed. M. Thumm and W. Wiesbeck, Univ. of Karlsruhe, Karlsruhe, pp 109-110 (2004).

[5] T. Idehara, I. Ogawa, S. Mitsudo, M. Pareyaslavets, N. Nishida, and K. Yoshida, "Development of frequency tunable, medium power gyrotrons (Gyrotron FU Series) as submillimeter wave radiation sources," IEEE Trans. Plasma Sci., **27**, 340-354 (1999).

[6] G. F. Brand, P. W. Fekete, K. Hong, K. J. Moore, and T. Idehara, "Operation of a tunable gyrotron at second harmonic of electron cyclotron frequency," Int. J. Electronics, **68**, 1099-1111 (1990).

[7] M. K. Hornstein, V. S. Bajaj, R. G. Griffin, and R. J. Temkin, "Continuous-wave operation of a 460-GHz second harmonic gyrotron oscillator," IEEE Trans. Plasma Sci., **34**, 524-533 (2006).

[8] I. Ogawa, K. Yoshisue, H. Ibe, T. Idehara, and K. Kawahata, "Long-pulse operation of a submillimeter wave gyrotron and its application to plasma scattering measurement," Rev. Sci. Instrum., **65**, 1778-1789 (1994).

[9] T. Tatsukawa, T. Maeda, H. Sasai, T. Idehara, M. Mekata, T. Saito, and T. Kanemaki, "ESR spectroscopy with a wide frequency range using a

gyrotron as a radiation power source," Int. J. Infrared and Millimeter Waves, **16**, 293-305 (1995).

[10] S. Mitsudo, Aripin, T. Matsuda, T. Kanemaki, and T. Idehara, "High power, frequency tunable, submillimeter wave ESR device using a gyrotron as a radiation source," Int. J. Infrared and Millimeter Waves, **21**,661-676 (2000).

[11] V. S. Bajaj, C. T. Farrar, M. K. Hornstein, I. Mastovsky, J. Vieregg, J. Bryant, B. Elena, K. E. Kreischer, R. J. Temkin, and R. G. Griffin, "Dynamic nuclear polarization at 9 T using a novel 250 GHz gyrotron microwave source, J. Magnetic Resonance, **160**, 85-90 (2003).

[12] T. Tatsukawa, A. Doi, M. Teranaka, H. Takashima, F. Goda, S. Watanabe, T. Idehara, T. Kanemaki, and T. Namba, "Microwave invasion though anti-reflecting layers of dielectrics at millimeter wave radiation to living bodies," Int. J. Infrared and Millimeter Waves, **26**, No. 4, 591-606 (2005)

[13] T. Idehara, S. Mitsudo, S. Sabchevski, M. Glyavin, and I. Ogawa, "Gyrotron FU series – current status of development and applications," Vacuum, **62**, 123-132 (2001).

[14] I. Ogawa, T. Idehara, S. Maekawa, W. Kasparek, G. F. Brand, "Conversion of gyrotron output into a gaussian beam using the far-field, Int. J. Infrared and Millimeter Waves, **20**, No. 5, 801-821 (1999).

[15] T. Idehara, H. Tsuchiya, O. Watanabe, La Agusu and S. Mitsudo, "The first experiment of a THz gyrotron with a pulse magnet," Int. J. Infrared and Millimeter Waves, **27**, 319 (2006).

[16] T. Saito, T. Idehara, S. Mitsudo, I. Ogawa, H. Hoshizuki, H. Murase, and K. Sakai, "Oscillation characteristic of CW 300 GHz gyrotron FU CW I," Conf. Diggest of the 2006 Joint 31th Int. Conf. on Infrared and MM Waves and 14th Int. Conf. on terahertz electronics, ed. S. C. Chen, W. Lu, J. Zhang, and W. B. Dou, Shanghai, China, p. 24 (2006).

[17] La Agusu, H. Murase, T. Idehara, T. Saito, S. Mitsudo, D. Takahashi, and T. Fujiwara, "Design of a 400 GHz gyrotron for DNP-NMR spectroscopy," Conf. Diggest of the 2006 Joint 31th Int. Conf. on Infrared and MM Waves and 14th Int. Conf. on terahertz electronics, ed. S. C. Chen, W. Lu, J. Zhang, and W. B. Dou, Shanghai, China, p. 82 (2006).

[18] T. Idehara, Y. Iwata, and I. Ogawa, "Observation of frequency-domain shift in a submillimeter wave gyrotron, "Int. J. Infrared and Millimeter Waves, **24**, 119-128 (2003).

[19] T. Hori, T. Idehara, H. Sasagawa, A. Kimura, I. Ogawa, and S. Mitsudo, "Relationship among frequency, temperature of the cooling water and beam current in submillimeter wave gyrotron FU-IV," Rev. Scientific Instruments, **76**, 023502 (2005).

[20] T. Idehara, I. Ogawa, S. Maeda, R. Pavlichenko, S. Mitsudo, D. Wagner, and M. Thumm, "Observation of mode patterns for high purity mode operation in the submillimeter wave gyrotron FU VA," Int. J. Infrared and Millimeter Waves, **23**, No. 9, 1287 (2002).

[21] A. N. Kuftin, V. K. Lygin, V. N. Manuilov, B. V. Raisky, E. A. Solujanova, Sh. E. Tsimiring, Theory of helical beams in gyrotrons, Int. J. Infrared and Millimeter Waves, **14**, 783-816 (1993).

[22] N. A. Zavolvsky, G. S. Nusinovich, and A. B. Pavelyev, "Stability of single mode oscillations and nonstationay processes in gyrotron with oversized low-quality resonators," *Gyrotrons*, Institute of Applied Physics, Academy of Sciences of the USSR, Gorky, Collection of scientific papers, Editor A. V. Gaponov-Grekhov, pp. 84-112 (1989).